

ish dopant–dopant interactions in the solid state, as well as systematic optimization of LED fabrication protocols.

### Experimental

LEDs were fabricated in the following manner. Indium tin oxide (ITO) substrates were cleaned by ultrasonication in detergent, acetone, and isopropanol. Cleaning was followed by a 5 min oxygen plasma etch at 100 W at 300 Torr of oxygen. After etching, poly(3,4-ethylenedioxythiophene) (PEDOT, Baytron P8000 from Bayer) was spin-cast at 3800 RPM in air. The substrates were baked at 110 °C in a nitrogen atmosphere to remove the water. The organic blends were spin-cast to get 100 nm thick films. The substrates were baked at 80 °C for 2 h after spin-casting the organic layer. Metalization of the cathodes was carried out at  $7 \times 10^{-7}$  Torr to deposit 80 nm of calcium and 130 nm of silver.

All LED testing was done under nitrogen atmosphere. LIV (LIV = luminance, current, voltage) data were acquired by inserting the substrate into a barium sulfate-coated integrating sphere with a radiometrically calibrated detector and sweeping the voltage while the current and radiant flux was measured. The exitance was calculated by dividing the radiant flux by the emitting area. The electroluminescence spectra were acquired using an Ocean Optics S2000 fiber optic spectrometer.

Cyclic voltammetric measurements were performed on an EG&G Princeton Applied Research model 273A potentiostat/galvanostat system using a standard three-electrode cell configuration. Electrolyte solutions utilized  $n\text{-Bu}_4\text{NPF}_6$  (0.10 M) in acetonitrile. The polymer or porphyrin films were coated on Pt or glassy carbon disk working electrodes by dipping the electrode into the corresponding solution and then drying in air. Pt wire and saturated calomel electrodes (SCE) were used respectively as counter and reference electrodes, while the ferrocene/ferricinium redox couple was utilized as an internal potentiometric standard. Scan rates in these experiments were 100 mV s<sup>-1</sup>.

Assuming the energy level of the ferrocene/ferricinium redox couple is 4.8 eV below the vacuum level, the potentiometrically derived HOMO and LUMO energy levels of the guests and hosts used in these experiments were plotted relative to vacuum. For polymers for which only reduction or oxidation potentials were obtained, their HOMO or LUMO levels were estimated from the combination of the cyclic voltammetric data and the optical bandgap (onset energy of the absorption spectrum); this method for estimating the valence and conduction band energies of conducting polymers has been discussed previously [21].

Received: April 7, 2003  
Final version: May 3, 2003

- [1] a) C. Wu, J. C. Sturm, R. A. Register, J. Tian, E. P. Dana, M. E. Thompson, *IEEE Trans. Electron Devices* **1997**, *44*, 1269. b) Y. Ohmori, Y. Hironaka, M. Yoshida, N. Tada, A. Fujii, K. Yoshino, *Synth. Met.* **1997**, *85*, 1241. c) C. W. Tang, S. A. VanSlyke, C. H. Chen, *J. Appl. Phys.* **1989**, *65*, 3610.
- [2] D. F. O'Brien, C. Giebeler, R. B. Fletcher, A. J. Cadby, L. C. Palilis, D. G. Lidzey, P. A. Lane, D. D. C. Bradley, W. Blau, *Synth. Met.* **2001**, *116*, 379.
- [3] V. Cleave, G. Yahioglu, P. Le Barny, R. H. Friend, N. Tessler, *Adv. Mater.* **1999**, *11*, 285.
- [4] X. Gong, M. R. Robinson, J. C. Ostrowski, D. Moses, G. C. Bazan, A. J. Heeger, *Adv. Mater.* **2002**, *14*, 581.
- [5] M. D. McGehee, T. Bergstedt, C. Zhang, A. P. Saab, M. O'Regan, G. C. Bazan, V. I. Srdanov, A. J. Heeger, *Adv. Mater.* **1999**, *11*, 1349.
- [6] R. G. Sun, Y. Z. Wang, Q. B. Zheng, H. J. Zhang, A. J. Epstein, *J. Appl. Phys.* **2000**, *87*, 7589.
- [7] a) L. H. Slooff, A. Polman, F. Cacialli, R. H. Friend, G. A. Hebbink, F. C. J. M. van Veggel, D. N. Reinhoudt, *Appl. Phys. Lett.* **2001**, *78*, 2122. b) B. S. Harrison, T. J. Foley, M. Bouguettaya, J. M. Boncella, R. J. Reynolds, K. S. Schanze, J. Shim, P. H. Holloway, G. Padmanaban, S. Ramakrishnan, *Appl. Phys. Lett.* **2001**, *79*, 3770. c) O. M. Khreis, W. P. Gillin, R. J. Curry, *J. Appl. Phys.* **2000**, *88*, 777.
- [8] a) R. G. Sun, Y. Z. Wang, Q. B. Zheng, H. J. Zhang, A. J. Epstein, *J. Appl. Phys.* **2000**, *87*, 7589. b) Y. Kawamura, Y. Wada, S. Yanagida, *Jpn. J. Appl. Phys.* **2001**, *40*, 350. c) R. J. Gurry, W. P. Gillin, *Curr. Opin. Solid State Mater. Sci.* **2001**, *5*, 481.
- [9] a) D. R. Baigent, P. J. Hamer, R. H. Friend, S. C. Moratti, A. B. Holmes, *Synth. Met.* **1995**, *71*, 2175. b) M. R. Anderson, M. Berggren, O. Inganäs, G. Gustafsson, J. C. Gustafsson-Carlberg, D. Selse, T. Hjertberg, O. Wennerstrom, *Macromolecules* **1995**, *28*, 7525.
- [10] a) H. Suzuki, *Appl. Phys. Lett.* **2000**, *76*, 1543. b) S. E. Shaheen, D. Vangeneugden, R. Kiebooms, D. Vanderzande, T. Fromherz, F. Padinger, C. J. Brabec, N. S. Sariciftci, *Synth. Met.* **2001**, *121*, 1583.

- [11] R. Englman, J. Jortner, *Mol. Phys.* **1970**, *18*, 145.
- [12] a) V. S.-Y. Lin, S. G. DiMugno, M. J. Therien, *Science* **1994**, *264*, 1105. b) V. S.-Y. Lin, M. J. Therien, *Chem. Eur. J.* **1995**, *1*, 645. c) R. Kumble, S. Palese, V. S.-Y. Lin, M. J. Therien, R. M. Hochstrasser, *J. Am. Chem. Soc.* **1998**, *120*, 11 489. d) R. Shediach, M. H. B. Gray, H. T. Uyeda, R. C. Johnson, J. T. Hupp, P. J. Angiolillo, M. J. Therien, *J. Am. Chem. Soc.* **2000**, *122*, 7017.
- [13] P. J. Angiolillo, V. S.-Y. Lin, J. M. Vanderkooi, M. J. Therien, *J. Am. Chem. Soc.* **1995**, *117*, 12 514.
- [14] J. T. Fletcher, M. J. Therien, *Inorg. Chem.* **2002**, *41*, 331.
- [15] K. Susumu, M. J. Therien, *J. Am. Chem. Soc.* **2002**, *124*, 8550.
- [16] H. T. Uyeda, V. S.-Y. Lin, S. A. Williams, T. Troxler, M. J. Therien, unpublished results.
- [17] T. Förster, *Discuss. Faraday Soc.* **1959**, *27*, 7.
- [18] The absolute emission energy of DD and DDD in the solid state vary as a function of the host matrix and the extent of guest loading.
- [19] J. Pommerehne, H. Vestweber, W. Guss, R. F. Mahrt, H. Bässler, M. Porsch, J. Daub, *Adv. Mater.* **1995**, *7*, 551.
- [20] N. J. Turro, *Modern Molecular Photochemistry*, University Science Books, Sausalito, CA **1991**.
- [21] Y. Li, Y. Cao, J. Gao, D. Wang, G. Yu, A. J. Heeger, *Synth. Met.* **1999**, *99*, 243.

## Generation of Uniform Colloidal Assemblies in Soft Microfluidic Devices\*\*

By Gi-Ra Yi, Todd Thorsen, Vinodhan N. Manoharan, Moon-Ja Hwang, Seog-Jin Jeon, David J. Pine,\* Stephan R. Quake, and Seung-Man Yang

Monodisperse spherical colloids such as polymer latexes and silica suspensions serve as model systems for practical colloidal materials or biological systems because of their uniform response to external electromagnetic and flow fields.<sup>[1]</sup> In particular, the uniform-sized colloidal assemblies have a number of potential applications such as paper-like displays, size-exclusion chromatography, photocatalyst supports, and nano-bar-

- [\*] Prof. D. J. Pine  
Department of Chemical Engineering and Materials  
Materials Research Laboratory, University of California  
Santa Barbara, CA 93106 (USA)  
E-mail: pine@mrl.ucsb.edu
- Dr. G.-R. Yi,<sup>[+]</sup> M.-J. Hwang, S.-J. Jeon, Prof. S.-M. Yang  
Department of Chemical and Biomolecular Engineering  
Korea Advanced Institute of Science and Technology  
373-1 Guseong-dong, Yuseong-gu, Daejeon 305-701 (Korea)
- Dr. T. Thorsen<sup>[++]</sup>  
Division of Chemistry and Chemical Engineering  
California Institute of Technology  
Pasadena, CA 91125(USA)
- V. N. Manoharan  
Department of Chemical Engineering  
University of California  
Santa Barbara, CA 93106 (USA)
- Prof. S. R. Quake  
Department of Applied Physics  
California Institute of Technology  
Pasadena, CA 91125(USA)

[+] Present address: Department of Chemical Engineering, University of California, Santa Barbara, CA 93106, USA.

[++] Present address: Department of Mechanical Engineering, Massachusetts Institute of Technology, Cambridge, MA 02139, USA.

[\*\*] This work was supported by the US NSF grant number CTS-0221809, the Brain Korea 21 Program, and the Korean National Nanotechnology Project. We also thank Prof. J. H. Hahn for helpful discussions on sorting experiments.

codes for the recognition of biological molecules. In addition, their self-organization with three-dimensional (3D) periodicity on the scale of optical wavelengths has received much attention as a promising route to 3D photonic bandgap (PBG) materials.<sup>[2,3]</sup> Recently, a few research groups have successfully prepared various organic or inorganic monodisperse colloidal assemblies with *non-spherical* shapes such as ellipsoids,<sup>[4]</sup> dumbbells,<sup>[5]</sup> and hollow spheres.<sup>[6,7]</sup> Their complexity may enable us to fabricate novel photonic bandgap materials, as well as to model real colloids with rather irregular structures. Meanwhile, another approach to structured colloidal assemblies has been developed by use of *spherical* colloid building units. For example, two-dimensional (2D) colloidal assemblies with well-defined size, shape, and structure can be obtained under 2D confinement in a patterned photoresist film.<sup>[8,9]</sup> Simple heterogeneous colloidal assemblies can be prepared using specific chemical or biochemical interactions between two types of monodisperse colloids.<sup>[10–12]</sup> Recently, the fabrication of 3D homogeneous colloidal assemblies with well-defined structure and shape has been reported.<sup>[13–20]</sup> However, it is still challenging to fabricate uniform 3D colloidal assemblies at *micrometer* length scales.

Here, we report a soft-lithography-based microfluidic approach to the fabrication of micrometer-sized 3D colloidal assemblies with narrow size distribution, in which monodisperse latex spheres are assembled into a regular arrangement. Our strategy begins with the generation of water-in-oil emulsions that contain the monodisperse latex spheres by using soft microfluidic devices developed by Thorsen et al. (see Fig. 1a).<sup>[21]</sup> Then, the water-in-oil emulsions are converted to uniform colloidal assemblies of latex spheres by slowly removing water from the aqueous emulsion droplets. The microfluidic device employed here is a very versatile tool compared with a standard cross-flow technique that produces a monodisperse emulsion by forcing the discontinuous phase into an open continuous phase through narrow pores.<sup>[22–26]</sup> The microfluidic device generates uniform emulsion drops at specific intervals by tearing off the tip of the incoming aqueous phase at the junction of two microfluidic channels as shown in Figure 1. In this flow configuration, the flow of the oil phase pushes to stretch the incoming aqueous suspension phase at the junction and the hydrodynamic stress tears an emulsion drop from the aqueous phase. In principle, all types of drop breakup modes can be realized in a suitably designed

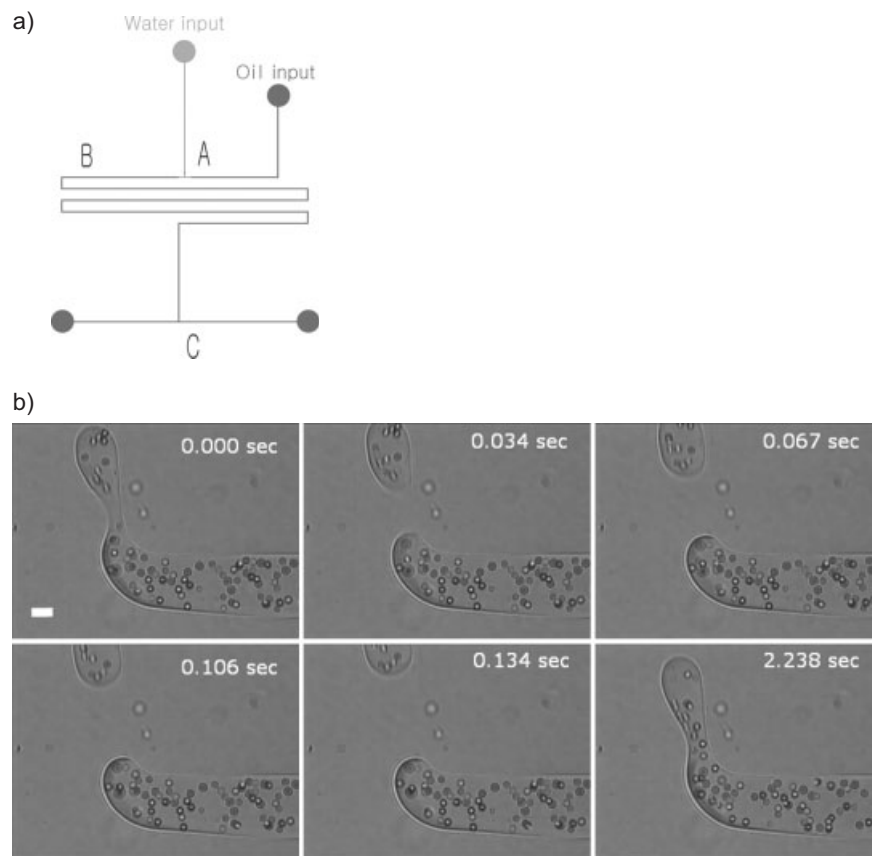


Fig. 1. a) Schematic of the microchannel for monodisperse suspension emulsion generation. Water droplets are created at junction A by the flow of oil and water into channel B and are subsequently collected at one of the outlets after passing through junction C. b) Optical images of the generation of monodisperse emulsion drops containing 2  $\mu\text{m}$  sized beads at junction A, depicted in (a). The pressures applied to the oil and the aqueous suspension reservoirs are 103 and 96 kPa, respectively. (Scale bar is 5  $\mu\text{m}$ ).

2D microchannel as proposed by theoretical investigation.<sup>[27]</sup> The formation of the aqueous emulsion drops can be characterized by the viscosity and flow-rate ratios of aqueous phase to oil phase and the capillary number, which is the ratio of the restoring surface tension to deforming shear stress. These dimensionless groups as well as the channel geometry are the primary parameters in determining the size of micrometer-scale emulsion drops and the generation frequency.

The uniform-sized emulsion droplets generated at the junction point travel along the oil phase capillary flow through the microchannel. In general, the flow in a microfluidic channel is laminar at low Reynolds numbers and consequently the emulsion droplets are moving in the same pattern as they are formed. Thorsen et al.<sup>[21]</sup> have examined various dynamic pattern formations of the emulsion drops by modifying the pressure of the aqueous phase relative to that of the oil phase, and showed that the emulsion drops kept traveling apart without coalescing under the condition where the inlet pressure of the aqueous phase is lower than that of the oil phase (for example, patterns B, C, and H in Fig. 3 of Thorsen et al.).<sup>[21]</sup> The segregated emulsion droplets suspended in the oil phase keep moving along the microchannel and shrink slowly as

water is absorbed in the oil phase (Fig. 2). As the particles are concentrated in an emulsion drop, they begin to order into a consolidated colloidal assembly (Fig. 2b). It is noteworthy that no stabilizer is necessary in the oil phase because the gen-

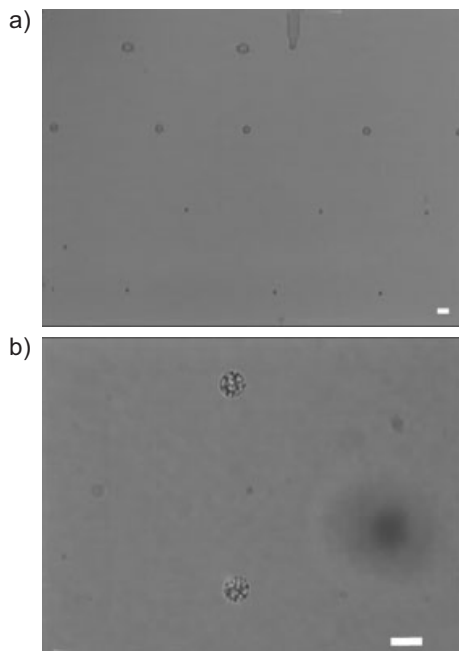


Fig. 2. a) Optical micrograph showing the size reduction of the aqueous droplets traveling down along the oil phase flow through the microchannel of the soft-microfluidic chips. Scale bar is 60  $\mu\text{m}$ . b) Optical image of the consolidated colloidal assemblies of the polystyrene latex particles, of which the diameter is about 1  $\mu\text{m}$ . (Scale bar is 5  $\mu\text{m}$ ).

erated droplets did not run into each other in the present laminar flow condition. The microfluidic control renders the consolidated particle assemblies stable against the collision-induced coalescence. Moreover, the absence of surfactant stabilizer on the oil–water interface facilitates the water absorption into the oil phase.

Polydimethylsiloxane (PDMS; Sylgard 184, Dow Corning), which is a basic material of the present soft microfluidic devices, is not compatible with most hydrocarbon oils. In particular, low-molecular-weight hydrocarbon oils are lethal to PDMS microfluidic devices. According to our test, silicone oil (purchased from Gelest) and fluorinated silicone oil (from ShinEtsu) are compatible with our PDMS. Additional requirements for the oil phase in our experiment are present: the oil should absorb water from the aqueous emulsion drops so that the particles can form regular assemblies in the emulsion droplets, and colloidal latex particles should reside in the droplets without escaping into the oil phase. In our previous work, we found that both silicone oil and fluorinated silicone oil satisfy these requirements for the present purpose. Meanwhile, other systems such as a mixture of mineral oil and surfactant cause the latex particles to escape from the emulsion drops to the oil phase and then the encapsulated droplets are destroyed spontaneously.

Meanwhile, water is perfectly compatible with PDMS chips. We found that the polymer latex particles in aqueous medium have failed to keep their stability in the microchannel because the latex particles have adsorbed on the PDMS wall. Presumably, this instability was caused by the deficiency in repulsive forces between the PDMS channel wall and the latex particles that were prepared by emulsifier-free emulsion polymerization. Therefore, we have added water-soluble surfactant into the aqueous suspension as stabilizer. We have tested several polymeric surfactants, including Tween 20 (Aldrich), hydrophilic methacrylate-graft-copolymer (Atlox4913; Uni-Qema), and triblock PEO–PPO–PEO copolymer (Pluronic P123, BASF; PEO = poly(ethylene oxide), PPO = poly(propylene oxide)), all of which were good enough for this purpose. The optical images in Figure 1b shows that particles does not adsorb on PDMS wall any more.

The number of captured particles  $N$  inside an emulsion droplet is a very important parameter for the internal structure of the colloidal assembly, especially for developing novel photonic crystals that will be fabricated by using the colloidal assemblies as building units. It can be seen from Figure 3 that the number of spherical latexes inside an aqueous droplet ex-

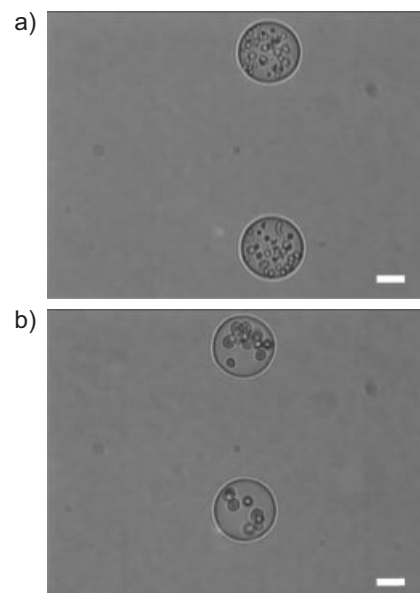


Fig. 3. Mono-sized suspension droplets containing 1  $\mu\text{m}$  (a) and 2  $\mu\text{m}$  (b) sized polystyrene beads. (Scale bars are 5  $\mu\text{m}$ ).

hibits statistical variation. When  $N$  is not large, the exact number of the captured particles can be determined from a 2D view captured in a video movie file.<sup>[28]</sup> Our results showed that the fluctuations relative to the average number were very small and within a few percent when the average number of the particles was as large as a few hundred. Therefore, the present microfluidic devices are quite useful for the fabrication of uniform colloidal assemblies with a relatively large number of constituent particles. These colloidal assemblies have great potential application, for example, as model colloids for complex colloidal particles such as erythrocyte in

blood vessels or as electronic inks for paper-like display if a binary mixture would be used as reported by Velev et al.<sup>[13]</sup> As expected, however, the fluctuations of  $N$  became large as the average number of the captured particles reduced (see Fig. 3b). In fact, the distribution of particles within a droplet produced in a given run obeys a Poisson distribution, as shown in Figure 4. In this case the mean number of particles per droplet is 4.3. The mean number of particles can be increased by increasing the concentration of particles in the feed stream. Consistent with what is expected for a random Poisson pro-

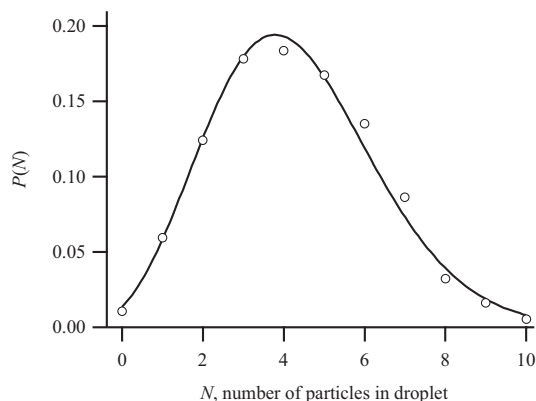


Fig. 4. Distribution of the number of particles inside a droplet produced in one run determined by manually counting the particles inside 185 separate droplets. The solid line is a fit to a Poisson distribution where the mean number of particles is 4.3.

cess, the width of the distribution relative to the mean narrows as  $N$  is increased. If a narrower distribution of particle number is desired, we would need to incorporate a subsequent process into the microfluidic device to sort out the colloidal assemblies by the number of the constituent particles. One possible candidate is a dielectrophoretic separation system or a microfluidic sorting device that is able to detect optically the number of embedded particles inside an emulsion drop. Ongoing experiments in our laboratory are designed to address this issue.

Typical microscopy images of the colloidal crystallites of 2  $\mu\text{m}$  polymer beads from our soft-lithography-based microfluidic devices are reproduced in Figures 5a–c. Also included for comparison are the model assemblies constructed by using 15 and 4 uniform-sized spheres, i.e.,  $N=4$  and 15. The internal structures of the colloidal assemblies can be identified by comparing with the model diagrams, especially when the number of the internal particles is small. Indeed, in these particular cases of  $N=4$  and 15, these pictures showed that the suspension particles were crystallized into defect-free colloidal assemblies inside the aqueous droplets if the right number of particles were encapsulated at the drop generation step.

A single junction produces on the order of 1–5 droplets per second or about 50–300 per minute. An advantage of a microfluidic method such as the one we report here is that it can readily be scaled up by putting many such devices on a single chip. It would not be difficult, for example, to fabricate hundreds or even thousands of junction points so that the rate of

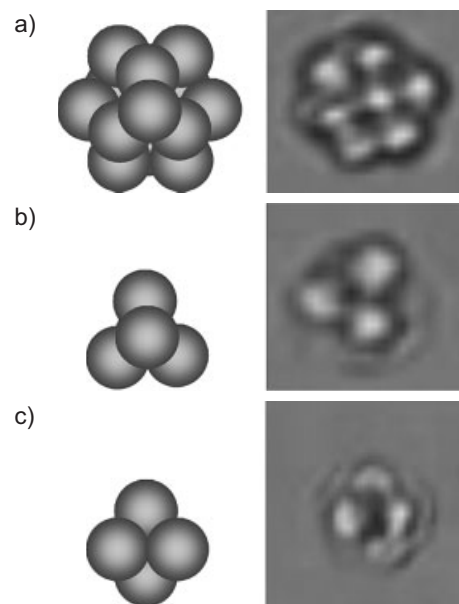


Fig. 5. Model assemblies (left) and optical images (right) of the prepared colloidal assemblies, which are composed of 15 polystyrene beads in (a) and 4 polystyrene beads in (b) and (c).

droplet production could be on the order of  $10^4$  droplets per second or even higher.

In summary, we have demonstrated that soft-lithography-based microfluidics and droplet break-off dynamics can be combined to produce uniform colloidal assemblies from a monodisperse suspension. Experimental results showed that colloidal assemblies with a reasonable uniformity were prepared and the uniformity was enhanced as the number of the embedded particles was increased. For colloidal assemblies with a smaller number of particles, the present microfluidic device has to be incorporated with a subsequent soft-microfluidic device to sort the assemblies by the number of the internal particles, which is under way in our research group. In addition, design of other type of microfluidic channels and microfluidic chip made out of more chemically inert materials are of potential interest for the fabrication of colloidal assemblies from non-aqueous suspension droplets and complex colloidal assemblies of multi-sized colloidal particles.

## Experimental

The 0.25  $\mu\text{m}$  diameter polystyrene beads were synthesized by surfactant-free emulsion polymerization [29], the 1  $\mu\text{m}$  diameter beads were purchased from Polysciences (Warrington, PA), and the 2  $\mu\text{m}$  diameter beads were synthesized by dispersion polymerization. The polystyrene beads were initially dispersed in ethanol, which was replaced by water to produce an aqueous suspension [30]. Silicone oil (KF-96) with a kinematic viscosity of 500 cSt was purchased from ShinEtsu; fluorinated silicone oil (FMS-123) was purchased from Gelest. The height of the photoresist mold on glass was measured by an alpha-step surface profiler.

The microfluidic devices employed in the present study were fabricated by a stepwise process; first, silicone prepolymer, polydimethylsiloxane, is poured on a silicon wafer mold containing positive-relief channels of a patterned photoresist (AZ9260, Clariant). Then, the prepolymer is cured at 80  $^{\circ}\text{C}$  for 40 min, and the replicated channels patterned in PDMS are completely covered by using a coverslip onto which a precured thin layer of PDMS is coated. In the final stage,

the coverslip adheres completely to the channel-patterned PDMS through an additional curing at again 80 °C for 1.5 h, which prevents leakage [31,32]. The measured channel dimensions are approximately 60 μm wide × 7 μm high, tapering to 35 μm × 6 μm in the region where the immiscible pair of aqueous and oil phases meet at the cross-flow junction (Fig. 1). The immiscible fluids are injected into the PDMS microfluidic devices from the pressurized reservoirs of the aqueous suspension and the silicone oil. The pressure is applied to the reservoirs with compressed nitrogen, and the device output channel is allowed to vent to atmosphere. All reported pressures are the gauge values.

Received: January 21, 2003  
Final version: April 18, 2003

- 
- [1] W. B. Russel, D. A. Saville, W. R. Schowalter, *Colloidal Dispersions*, Cambridge University Press, New York **1989**.
- [2] A. D. Dinsmore, J. C. Crocker, A. G. Yodh, *Curr. Opin. Colloid Interface Sci.* **1998**, 3, 5.
- [3] O. D. Velev, E. W. Kaler, *Adv. Mater.* **2000**, 12, 531.
- [4] E. Snoeks, A. van Blaaderen, T. van Dillen, C. M. van Kata, M. L. Bronersma, A. Polman, *Adv. Mater.* **2000**, 12, 1511.
- [5] Y. Lu, Y. Yin, Y. Xia, *Adv. Mater.* **2000**, 13, 415.
- [6] P. Jiang, J. F. Bertone, V. K. Colvin, *Science* **2001**, 291, 453.
- [7] Z. Zhong, Y. Yin, B. Gates, Y. Xia, *Adv. Mater.* **2000**, 12, 206.
- [8] Y. Yin, Y. Lu, Y. Xia, *J. Am. Chem. Soc.* **2001**, 123, 771.
- [9] Y. Yin, Y. Xia, *Adv. Mater.* **2001**, 13, 267.
- [10] M. S. Fleming, T. K. Mandal, D. R. Walt, *Chem. Mater.* **2001**, 13, 2210.
- [11] A. L. Hiddessen, S. D. Rodgers, D. A. Weitz, D. A. Hammer, *Langmuir* **2000**, 16, 9744.
- [12] K. Furusawa, O. D. Velev, *Colloids Surf. A* **1999**, 159, 359.
- [13] O. D. Velev, A. M. Lenhoff, E. W. Kaler, *Science* **2000**, 287, 2240.
- [14] G.-R. Yi, J. H. Moon, S.-M. Yang, *Adv. Mater.* **2001**, 13, 1185.
- [15] O. D. Velev, K. Nagayama, *Langmuir* **1997**, 13, 1856.
- [16] G.-R. Yi, J. H. Moon, S.-M. Yang, *Chem. Mater.* **2001**, 13, 2613.
- [17] Y. A. Vlasov, X. Z. Bo, J. C. Sturm, D. J. Norris, *Nature* **2001**, 414, 289.
- [18] S. M. Yang, H. Miguez, G. A. Ozin, *Adv. Funct. Mater.* **2002**, 12, 425.
- [19] G. A. Ozin, S. M. Yang, *Adv. Funct. Mater.* **2001**, 11, 95.
- [20] S. M. Yang, G. A. Ozin, *Chem. Commun.* **2000**, 24, 2507.
- [21] T. Thorsen, R. W. Roberts, F. H. Arnold, S. R. Quake, *Phys. Rev. Lett.* **2001**, 86, 4163.
- [22] P. B. Umbanhowar, V. Prasad, D. A. Weitz, *Langmuir* **2000**, 16, 347.
- [23] B. Ambravaneswaran, S. D. Philips, O. A. Basaran, *Phys. Rev. Lett.* **2000**, 85, 5332.
- [24] I. G. Loscertales, A. Barrero, I. Guerrero, R. Cortijo, M. Marquez, A. M. Ganan-Calvo, *Science* **2002**, 295, 1695.
- [25] S. M. Joscelyne, G. Tragardh, *J. Membrane Sci.* **2000**, 169, 107.
- [26] S. Sugiura, M. Nakajima, J. Tong, H. Nabetani, M. Seki, *J. Colloid Interface Sci.* **2000**, 277, 95.
- [27] G.-R. Yi, S.-J. Jeon, T. Thorsen, V. N. Manoharan, S. R. Quake, D. J. Pine, S. M. Yang, *Synth. Met.* **2003**, in press.
- [28] S. Middleman, *Modeling Axisymmetric Flows: Dynamics of Films, Jets, and Drops*, Academic Press, New York **1995**.
- [29] J. H. Kim, M. Chainey, M. S. El-Aasser, J. W. Vanderhoff, *J. Polym. Sci., Part A: Polym. Chem.* **1989**, 27, 3187.
- [30] Y. Y. Lu, M. S. El-Aasser, J. W. Vanderhoff, *J. Polym. Sci., Part A: Polym. Chem.* **1990**, 28, 2569.
- [31] M. A. Unger, H.-P. Chou, T. Thorsen, A. Scherer, S. R. Quake, *Science* **2000**, 288, 113.
- [32] S. R. Quake, A. Scherer, *Science* **2000**, 290, 1536.
-